DOI:
10.1103/PhysRevLett.121.193901

Document Version
Peer reviewed version

Interferometric evanescent wave excitation of nano-antenna for ultra-sensitive displacement and phase metrology

Lei Wei,* Anatoly V. Zayats, and Francisco J. Rodríguez-Fortuño
Department of Physics, King's College London, Strand, London, WC2R 2LS, United Kingdom
(Dated: October 15, 2018)

We propose a method for ultra-sensitive displacement and phase measurements based on a nano-antenna illuminated with interfering evanescent waves. We show that with a proper nano-antenna design, tiny displacements and relative phase variations can be converted into changes of the scattering direction in the Fourier space. These sensitive changes stem from the strong position dependence of the orientation of the purely-imaginary Poynting vector produced in the interference pattern of evanescent waves. Using strongly confined evanescent standing waves, high sensitivity is demonstrated on the nano-antenna's zero-scattering direction, which varies linearly with displacement over a wide range. With weakly confined evanescent wave interference, even higher sensitivity to tiny displacement or phase changes can be reached near a particular location. The high sensitivity of the proposed method can form the basis for many metrology applications. Furthermore, this concept demonstrates the importance of the imaginary part of the Poynting vector, a property that is related to reactive power and is often ignored in photonics.

PACS numbers: 42.25.Hz, 42.25.Fx, 06.20.-f, 42.30.Kq,42.62.Eh

Sensitive optical metrology has been an enabling technology for modern science and engineering. Interferometric methods[1] are widely deployed for measuring the relative phase differences introduced by tiny physical displacements. The giant Michelson interferometer of LIGO that enables the detection of gravitational waves demonstrates the power of this technique[2]. Another technique to measure displacements is based on differential detection of beam deflections, which offers similar fundamental detection limits[3, 4]. These techniques form invaluable tools for applications that require sub-nm positioning precisions, like single molecules tracking[5–7], force sensing[8–11], localization nanoscopy[12] as well as overlay metrology for the semiconductor industry[13].

Apart from the evolving instrumentation, further advances have been made by the introduction of new concepts such as squeezed light[14, 15] and weak value amplification[16, 17]. With the development of beam shaping and nanofabrication, a new position sensing concept that involves the interaction of structured light and structured matter such as optical nano-antennas has also been demonstrated in recent years[18–22]. Nano-antennas that support both electric and magnetic modes, like high index dielectric nanoparticles, are of special interest recently[23–26] as their scattering can be shaped by the full vectorial nature of the electromagnetic (EM) excitation field[27–30]. Even in the simplest case of a dipolar nanoparticle, the induced electric dipole (ED) moment $\mathbf{p}$ and magnetic dipole (MD) moment $\mathbf{m}$ can interfere and result in uni-directional scattering. This occurs when Kerker's condition [31] is fulfilled, giving rise to the Huygens dipoles, in which the ED and MD moments are orthogonal to each other and their amplitudes are related by $\mathrm{p} = \mathrm{m}/c$ [18, 32], with c being the speed of light. Furthermore, the excitation field can be designed so that this directional scattering condition occurs only at certain locations in the field landscape[18–21]. Moving the particle slightly away from these locations will diminish the scattering directionality and the relative displacement can therefore be measured. For instance, using tightly focused vector beams as excitation fields, relative displacement down to Ångström level has been demonstrated[21] with a differential detection of the scattering pattern at the back focal plane (i.e. the k-space). Standing waves formed by counter-propagating beams in free space have been proposed as excitation fields for a metallic nanowire[20]. This method predicts theoretically ultra high relative displacement sensitivity around the nodal point where the electric field is zero but magnetic field is at its maximum. Being of extremely weak MD polarizability, the metallic nanowire serves an ideal nano-antenna realisation to fulfil the Kerker's condition in the close vicinity of the nodal point. As the nanowire moves across the point, its uni-directional scattering switches direction, and the closer the position to the nodal point, the higher the sensitivity is. However, this advantage is at the same time its disadvantage: due to working at the node, there is an extremely weak total scattering power which is difficult to detect. In addition, both free space focused beams and standing wave excitations suffer from the fact that the unwanted incident light enters the detection k-space. In order to detect the pure directional scattering of the nanoparticle, the k-space influenced by both the incident and scattered light is often cropped[18, 21], with a loss of useful information. Finally, these methods have a limited spatial range because high displacement sensitivity exists only near the locations of optimal directionality.

In this Letter, we propose a technique which overcomes all of these drawbacks. We exploit the unique topology of

the Poynting vector in the interference pattern of evanescent waves. By using the interfering evanescent waves as excitation fields for dipolar nano-antennas, the transverse displacement or relative phase difference is translated into angular changes in the scattering momentum space with the whole k-space being accessible. We further show that this approach can achieve not only extremely high displacement and phase sensitivity around certain positions, but also allows relatively high and linear displacement sensitivity over a wide range.

Different from free propagating waves, evanescent waves exhibit unique properties such as transverse spin angular momentum and intrinsic transverse spin-momentum locking[33]. A nanoparticle placed inside them acts as an antenna that converts local EM fields into far-field scattering. The special properties of evanescent waves used as excitation fields enable effective directional control of the nano-antenna's scattering[34] with applications ranging from tunable displays[35] to the generation of interesting optical forces[36, 37]. Interferometric evanescent waves have been used as structured illumination in Total Internal Reflection Fluorescence (TIRF) microscopy which doubles the imaging resolution and improves the contrast by minimizing the amount of incident light going into the detector[38]. Its electromagnetic properties are yet to be fully exploited, and combined with designer nano-antennas may unleash its full potential in measuring deeply sub-wavelength displacements and tiny phase changes.

Evanescent standing waves can be set up at an interface by illuminating with two transverse magnetic (TM or p) polarized incident plane waves $\mathbf{E}_\mathbf{p}^+$ and $\mathbf{E}_\mathbf{p}^-$ from a higher refractive index substrate above the critical angle (Fig. 1(a)). Consider two incident plane waves with opposite transverse wavevectors $\pm k_\parallel$ having exactly the same amplitude but a phase difference $\Delta\phi$. Assuming $\varepsilon_1 = 1$ and $\varepsilon_2 > \varepsilon_1$, the fields of the interfering evanescent wave can be written as:

$$\begin{aligned}\mathbf{E} &= \left[0, -\frac{\gamma_z}{k_0}\cos(k_\parallel y + \Delta\phi/2), \frac{k_\parallel}{k_0}\sin(k_\parallel y + \Delta\phi/2)\right] \\ &\quad \times 2\mathrm{i}E_p\exp(-\gamma_z z), \\ \mathbf{H} &= \left[\frac{1}{Z_0}\cos(k_\parallel y + \Delta\phi/2), 0, 0\right] \times 2E_p\exp(-\gamma_z z), \quad (1)\end{aligned}$$

where $k_0 = 2\pi/\lambda$ is the wavevector of incoming light, Z_0 is the impedance in vacuum and $\gamma_z = \sqrt{k_\parallel^2 - k_0^2}$ is the imaginary part of the z component of the wave-vector. Here, a time dependence of $e^{-\mathrm{i}\omega t}$ is assumed.

A single TM polarized evanescent wave has a real time-averaged Poynting vector component S_y along the propagation direction and an imaginary Poynting vector component $S_z \geq 0$ along the direction of evanescent decay[34], while both components are invariant in the y direction. In contrast, the standing wave interference of two TM polarized evanescent waves shown in Eq. (1) results in a purely imaginary time-averaged Poynting vector $\mathbf{S} = \frac{1}{2}(\mathbf{E} \times \mathbf{H}^*)$ in both y and z directions:

$$\begin{aligned}\mathbf{S} &= \left[0, \frac{k_\parallel}{k_0}\sin(2k_\parallel y + \Delta\phi), \frac{\gamma_z}{k_0}\left(1 + \cos(2k_\parallel y + \Delta\phi)\right)\right] \\ &\quad \times \mathrm{i}\frac{E_p^2}{Z_0}\exp(-2\gamma_z z), \quad (2)\end{aligned}$$

and the orientation of the vector $\mathbf{S}$ strongly depends on the transverse location y. At any height z, the direction of the imaginary part of the Poynting vector $\Im\{\mathbf{S}\}$ can be determined by:

$$\tan\theta_\mathrm{s} = \frac{S_z}{S_y} = \frac{\gamma_z}{k_\parallel}\frac{\cos(k_\parallel y + \Delta\phi/2)}{\sin(k_\parallel y + \Delta\phi/2)}, \quad (3)$$

where θ_s is the angle between $+\hat{\mathbf{y}}$ and the imaginary part of the Poynting vector $\Im\{\mathbf{S}\}$. Fig. 1(b) and (c) show two distinctively different scenarios of the Poynting vector's dependences on the transverse position y inside the standing waves. Fig. 1(b) represents the case with $k_\parallel/k_0 = 2$ being relatively large while Fig. 1(c) represents the case with $k_\parallel/k_0 = 1.01$, corresponding to illumination just above the critical angle. A nano-antenna

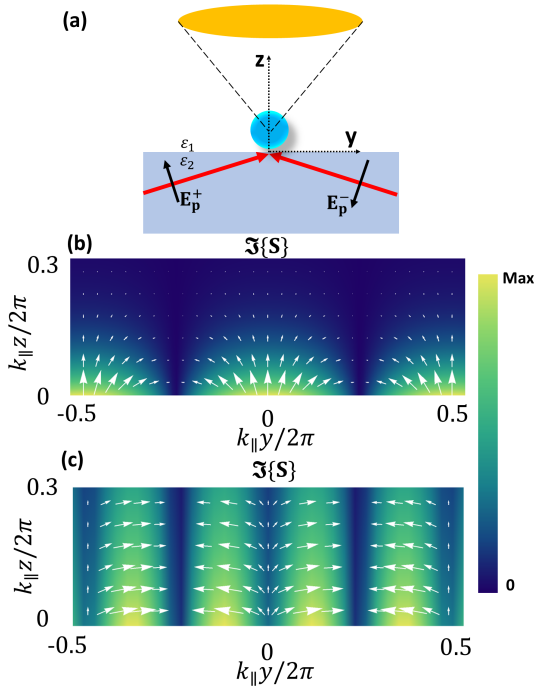

FIG. 1. (a). A dipolar nanoparticle is illuminated by two counter-propagating TM polarized evanescent waves. The scattering of the particle is measured at the back focal plane of a lens, i.e. in the Fourier k-space. (b, c) The purely-imaginary Poynting vector (color represents its magnitude and white arrows its orientation) of the standing wave due to the interference of two evanescent waves with opposite transverse wavevectors $\pm k_\parallel = \pm 2k_0$ (b) and $\pm k_\parallel = \pm 1.01k_0$ (c), where the phase difference between the two waves is set to $\Delta\phi = 0$.

can be used as a local probe of the fast changing Poynting vector to detect the displacement or phase changes by measuring its scattering. The sensitivity of this technique will depend on how fast θ_s changes with respect to location y. As can be derived from Eq. (3), in the limiting case of illumination well above the critical angle, we have $k_\parallel/k_0 \gg 1$ and $\gamma_z/k_\parallel \to 1$:

$$\frac{\mathrm{d}\theta_s}{dy} \approx -k_\parallel, \tag{4}$$

where the angle θ_s is changing linearly with the transverse position y across the entire period of the standing wave in Fig. 1(b). In the limiting case that $k_\parallel/k_0$ is slightly above one (and, therefore, γ_z/k_0 is slightly above zero), the angle of the purely-imaginary Poynting vector θ_s varies in a highly nonlinear manner along y and its rate of change depends strongly on the transverse location (Fig. 1(c)). For the fields at a position near $k_\parallel y/2\pi = 1/4$, one can derive from Eq. (3) that

$$\frac{\mathrm{d}\theta_s}{dy}|_{y\to\pi/(2k_\parallel)} = -\gamma_z, \tag{5}$$

which means the Poynting vector is changing orientation very slowly around such location. However, for the fields at a position very near $y = 0$, one has:

$$\frac{\mathrm{d}\theta_s}{dy}|_{y\to 0} = -\frac{k_\parallel^2}{\gamma_z}, \tag{6}$$

where the purely-imaginary Poynting vector is changing at an extremely high rate around $y = 0$ as $\gamma_z \to 0$.

As a probe, we consider a nano-antenna with both electric and magnetic responses. Though optical magnetism is rare in natural bulk materials, it has been demonstrated recently in nanostructures such as core-shell nanoparticles or nanospheres/nanowires made of high index dielectric materials like Si or Ge [20, 23–31]. These last examples are particularly suitable for our proposal as long as their dipole modes dominate in the spectral region of interest. For simplicity in explaining the concept of displacement metrology with interferometric evanescent waves, we further neglect the substrate's effect on the particle's scattering. Under such assumptions, the scattering of the nanoparticle is equivalent to the radiation of a source with respectively induced ED and MD moments $\mathbf{p} = \alpha_e\mathbf{E}$ and $\mathbf{m} = \alpha_m\mathbf{H}$, where $\alpha_e = \frac{i6\pi\varepsilon_0}{k_0^3}a_1$ and $\alpha_m = \frac{i6\pi}{k_0^3}b_1$ are the ED and MD polarizabilities respectively [39, 40], a_1 and b_1 are the Mie coefficients of the ED and MD modes respectively [41], ε_0 is the vacuum permittivity, and $\mathbf{E}$ and $\mathbf{H}$ are the incident interferometric evanescent fields in Eq. (1) at the center of the nanoparticle. The interference of the radiation fields of the induced ED and MD could result in directional scattering under certain conditions. The preferred scattering direction can be shown [39] to be always along the direction of $\Re\{\mathbf{p}\times\mathbf{m}^*\} = \Re\{\alpha_e\alpha_m^*\}\Re\{\mathbf{E}\times\mathbf{H}^*\} - \Im\{\alpha_e\alpha_m^*\}\Im\{\mathbf{E}\times\mathbf{H}^*\}$. When illuminated by the interfering evanescent fields in Eq. (1) whose Poynting vectors are purely imaginary, the preferred scattering direction is completely determined by the nano-antenna's dipolar polarizablities $\Im\{\alpha_e\alpha_m^*\}$ and the imaginary part of the Poynting vector $\Im\{\mathbf{S}\}$, in contrast to conventional plane wave illumination. We shall show later that with a proper choice of nano-antennas, the purely-imaginary Poynting vector, a property often ignored in photonics, can be used to devise a sensitive means to measure lateral displacements and phases by detecting scattering changes in the Fourier k-space.

We will first consider a dipolar nanoparticle placed in the interference field shown in Fig. 1(b) of two TM-polarized evanescent waves with relatively large transverse wavevectors $\pm k_\parallel = \pm 2k_0$ and a phase difference $\Delta\phi = 0$. Consider a particle with Mie coefficients fulfilling the condition $a_1 = (-\mathrm{i}k_0/\gamma_z)b_1$, realistic implementations of which were proposed in Ref. [34]. It can be shown from Eq. (1) that Kerker's condition is satisfied, independent of the position, such that the transverse components of the induced ED and MD always fulfil the relation $p_y = -m_x/c$. As a result, the scattering of the nanoparticle along the $-\hat{\mathbf{z}}$ direction is fixed to be zero no matter where it is located in the standing wave. More generally, the scattering cross section along any direction $\hat{\mathbf{k}}$ can be found proportional to $|\mathbf{p}^*\cdot\tilde{\mathbf{E}}_{\mathbf{k}} + \mathbf{m}^*\cdot\mu_0\tilde{\mathbf{H}}_{\mathbf{k}}|^2$, following Fermi's golden rule [42] which determines the coupling strength of the induced dipoles to the plane wave field vectors $[\tilde{\mathbf{E}}_{\mathbf{k}}, \tilde{\mathbf{H}}_{\mathbf{k}}]$ along wavevector $\mathbf{k}$.

In the $k_x = 0$ plane, due to the TM nature of the excitation field, the induced dipoles can only couple to the TM-polarized fields. The field vectors of the TM-polarized field propagating along $\mathbf{k} = (0, k_y, k_z) = (0, k_0\cos\theta, k_0\sin\theta)$ can be expressed as $\tilde{\mathbf{E}}_{\mathrm{TM},\mathbf{k}} = (0, -\sin\theta, \cos\theta)$ and $\tilde{\mathbf{H}}_{\mathrm{TM},\mathbf{k}} = (1/Z_0, 0, 0)$, where θ is the angle from $+\hat{\mathbf{y}}$ to $\mathbf{k}$ as defined in Fig. 2. By solving $\mathbf{p}^*\cdot\tilde{\mathbf{E}}_{\mathrm{TM},\mathbf{k}} + \mathbf{m}^*\cdot\mu_0\tilde{\mathbf{H}}_{\mathrm{TM},\mathbf{k}} = 0$, we can explicitly find two directions of zero scattering: one is fixed at $-\hat{\mathbf{z}}$ which is independent of y and the other directly related to the direction of the purely-imaginary Poynting vector:

$$\theta = 2\theta_s + \frac{2m+1}{2}\pi, \;\; m \text{ is integer}, \tag{7}$$

which, just as the Poynting vector, is highly dependent on the transverse location y. It is easy to observe from Eq. (7) that this zero scattering direction doubles the sensitivity of the Poynting vector to displacement changes ($\frac{\mathrm{d}\theta}{\mathrm{d}y} = 2\frac{\mathrm{d}\theta_s}{\mathrm{d}y}$). This can also be understood by the fact that these two zero scattering directions are symmetric with respect to the Poynting vector, so by locking one direction to $-\hat{\mathbf{z}}$, the other one rotates at twice the rotation angle of the symmetry axis, i.e., the Poynting vector.

Fig. 2 demonstrates how this concept applies to dis-

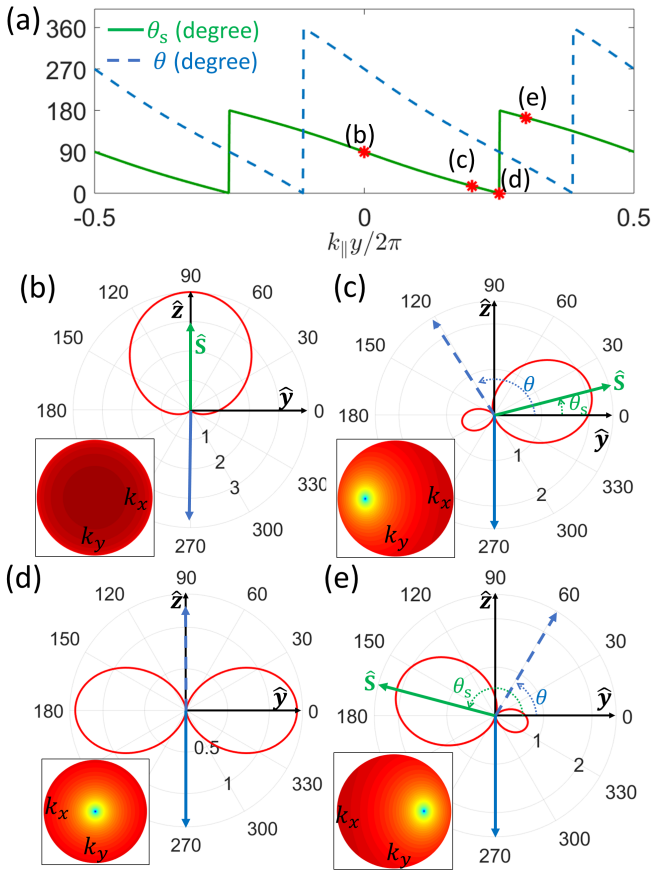

FIG. 2. (a). The y-dependence of of θ_s (the angle from $+\hat{\mathbf{y}}$ to the purely-imaginary Poynting vector of the interfering evanescent field shown in Fig. 1(b)) and θ (the angle from $+\hat{\mathbf{y}}$ to the particle's zero scattering direction). The scattering patterns of a dipolar particle are shown(the ED and MD coefficients fulfil $a_1 = \frac{-i}{\sqrt{3}} b_1$) placed at various locations: (b). $y = 0$, (c). $y = \lambda/4 - \lambda/40$, (d). $y = \lambda/4$; (e). $y = \lambda/4 + \lambda/40$. The green solid arrows represent the Poynting vectors, the blue solid arrow represents the fixed zero scattering direction $-\hat{\mathbf{z}}$, the blue dashed arrows represent the other zero scattering direction, while the insets in (b)-(e) show the scattering pattern (logarithm $\log_{10}$ scale, dark red for maximum while deep blue represents zero scattering) in the k-space of the Fourier lens above the nanoparticle.

placement metrology with Fig. 2(a) showing the y-dependence of the Poynting vector angle θ_s and the zero scattering direction angle θ, while Fig. 2(b)-(e) show the scattering patterns of the nano-antenna at various transverse locations of the interference field. At location $y = 0$, the scattering pattern in Fig. 2(b) exhibits the zero-scattering direction only along $-\hat{\mathbf{z}}$, with the maximum scattering observed along the direction of the purely-imaginary Poynting vector in the k-space of a lens above the nanoparticle. More interestingly, in the region $\pi/4 < k_\parallel y < 3\pi/4$, one observes the zero-scattering direction rapidly moving with y in the upper half of the Fourier space of the lens. The scattering appears as the one of a vertical electric dipole at the location $y = \lambda/4$, with zero-scattering along $+\hat{\mathbf{z}}$. With displacements of $\Delta y = \pm\lambda/40$ around $y = \lambda/4$, as shown in Fig. 2(c) and (e), respectively, the changes of zero-scattering angle $\Delta\theta = \mp 31.43°$ are introduced in the Fourier k-space. This corresponds to a sensitivity $\Delta\theta/\Delta y$ about $-1257.2°/\lambda$, which means a change of 1° in the zero-scattering direction can resolve a displacement of $\lambda/1257.2$. Using even larger $k_\parallel/k_0$, the sensitivity can reach up to $-(\frac{k_\parallel}{k_0})720°/\lambda$. Additionally, both θ_s and θ exhibit nearly linear relations with y (Fig. 2(a)) as expected from Eq. (4). This linear relation with y enables the detection of deep-subwavelength displacements as well as the displacement direction over wide ranges.

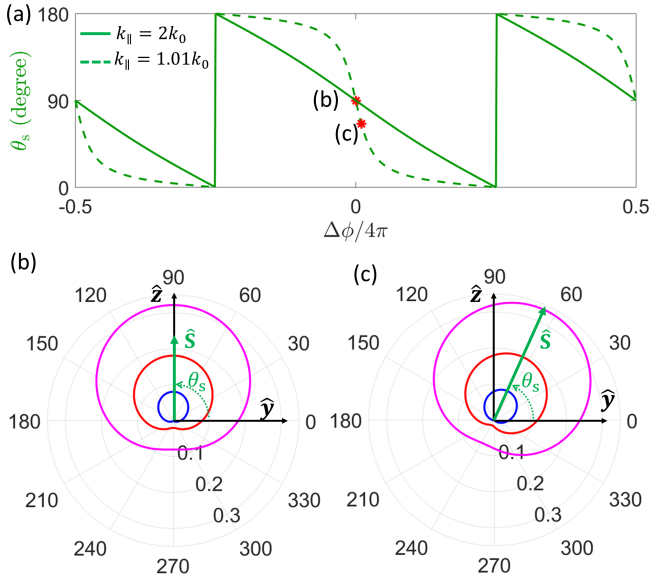

FIG. 3. (a). The dependence of the purely-imaginary Poynting vector angle θ_s on the relative phase difference $\Delta\phi$ at a fixed location $y = 0$ of the interferometric evanescent field with $\pm k_\parallel = \pm 2k_0$ and $\pm k_\parallel = \pm 1.01k_0$, respectively. The scattering patterns are shown for a dipolar particle placed at $y = 0$ of the interfering fields with different relative phases: (b) $\Delta\phi = 0$ and (c) $\Delta\phi = \pi/25$. The radiation patterns plotted in colours correspond to nanoparticles with fixed electric dipole but different magnetic dipole Mie coefficients: $b_1 = \mathrm{i}\frac{\gamma_z}{k_0} a_1$ (blue), $b_1 = 2\mathrm{i}\frac{\gamma_z}{k_0} a_1$ (red) and $b_1 = 3\mathrm{i}\frac{\gamma_z}{k_0} a_1$ (magenta), where $\gamma_z = 0.142k_0$.

As a second example, we investigate the use of weakly confined evanescent standing waves as shown in Fig. 1(c) for ultra-sensitive phase measurements. At a fixed location, the Poynting vector direction of an evanescent standing wave with $k_\parallel = 1.01k_0$ responds even more sensitively to relative phase changes of the two interfering beams. The principle is identical, because a relative phase difference of $\Delta\phi$ between the two interfering beams is equivalent to a displacement $y = \Delta\phi/2k_\parallel$. One can derive from Eq. (6) that, for small phase changes, the

sensitivity corresponds to

$$\frac{\mathrm{d}\theta_\mathrm{s}}{d\Delta\phi}|_{\Delta\phi\to 0} = -\frac{k_\parallel}{2\gamma_z}. \quad (8)$$

For a dipolar nanoparticle placed at the fixed location $y = 0$ of the interference field with $k_\parallel/k_0 = 1.01$, a 24.25° rotation of the maximum scattering direction in the upper k-space is introduced by a relative phase change of $\pi/25$ rad which is equivalent to a displacement of only $\lambda/101$ as shown in Fig. 3(b,c). With smaller γ_z/k_0, even higher sensitivity can be expected. One might think that this comes at a price: if Kerker's condition were to be met with such excitation field at $y = 0$, following Eq. (1), the nanoparticle would need to have polarizabilities that fulfil $b_1 = \mathrm{i}\frac{\gamma_z}{k_0}a_1$, resulting in a weak total scattering cross-section proportional to $(\gamma_z/k_0)^2$. However, since in this case only the preferred scattering direction, aligned to the purely-imaginary Poynting vector, is relevant for the detection in k-space, the Kerker's condition is not strictly required. As is shown in Fig. 3(b) and (c), by using particles with larger $|b_1/a_1|$, the scattering power can be greatly improved without diminishing the sensitivity.

The proposed method exploits the full electromagnetic vector field nature of the structured illumination formed by interfering evanescent waves. By using a dipolar nano-antenna with both electric and magnetic responses, the fast-varying purely-imaginary Poynting vector due to tiny displacement and phase variations is converted into sensitive scattering changes in the Fourier k-space. We show that using the excitation field formed by strongly confined evanescent standing waves, high sensitivity of the zero scattering direction with displacement can be observed over a long range. Using interference patterns of weakly confined evanescent waves, even higher sensitivity can be reached with tiny relative phase changes. The high sensitivity to displacement and phase changes, as demonstrated by this work, can form the basis for many applications including single molecule tracking, quantum metrology, wafer overlay and nano-optomechanical systems. Furthermore, the ultra-sensitive phase detection concept may also find applications in the area of bio-/chemical sensing to detect the phase variations introduced by environmental perturbations, like gases, biological binding or chemical reactions.

Acknowledgement: This work was supported by European Research Council Starting Grant ERC-2016-STG-714151-PSINFONI and the ERC iCOMM project. A.Z. acknowledges support from the Royal Society and the Wolfson Foundation.

* lei.wei@kcl.ac.uk

[1] N. Bobroff, Meas. Sci. Technol. **4**, 907 (1993).
[2] B. Abott *et al.*, Phys. Rev. Lett. **116**, 061102 (2016).
[3] C. A. J. Putman, B. G. De Grooth, *et al.*, J. of Appl. Phys. **72**, 6 (1992).
[4] S. M. Barnett, C. Fabre, and A. Maître, Eur. Phys. J. D **22**, 513 (2002).
[5] J. Gelles, B. J. Schnapp, and M. P. Sheetz, Nature **331**, 450 (1988).
[6] J. Ortega Arroyo and P. Kukura, Nature Photonics **10**, 11 (2015).
[7] F. Balzarotti, Y. Eilers, *et al.*, Science **355**, 601 (2017).
[8] G. Meyer and N. M. Amer, Appl. Phys. Lett. **53**, 1045 (1988).
[9] B. Sanii and P. D. Ashby, Phys. Rev. Lett. **104**, 147203 (2010).
[10] A. Gloppe *et al.*, Nature Nanotech. **9**, 920 (2014).
[11] V. Blūms *et al.*, Sci. Adv. **4**, eaao4453 (2018).
[12] L. Nugent-Glandorf and T. T. Perkins, Optics Lett. **29**, 2611 (2004).
[13] A. J. den Boef, Surf. Topogr.: Metrol. Prop. **4**, 023001 (2016).
[14] N. Treps, U. Andersen, *et al.*, Phys. Rev. Lett. **88**, 203601 (2002).
[15] R. C. Pooser and B. Lawrie, Optica **2**, 393 (2015).
[16] P. B. Dixon, D. J. Starling, A. N. Jordan, and J. C. Howell, Phys. Rev. Lett. **102**, 173601 (2009).
[17] M. D. Turner *et al.*, Optics Lett. **36**, 1479 (2011).
[18] M. Neugebauer *et al.*, Nature Comm. **7**, 11286 (2016).
[19] Z. Xi, L. Wei, A. J. L. Adam, H. P. Urbach, and L. Du, Phys. Rev. Lett. **117**, 113903 (2016).
[20] Z. Xi and H. P. Urbach, Phys. Rev. Lett. **119**, 053902 (2017).
[21] A. Bag, M. Neugebauer, *et al.*, arXiv:1804.10176.
[22] L. Du, A. Yang, A. V. Zayats, and X. C. Yuan, arXiv:1806.04827.
[23] A. I. Kuznetsov *et al.*, Sci. Rep. **2**, 492 (2012).
[24] S. Person *et al.*, Nano Lett. **13**, 1806 (2013).
[25] Y. H. Fu *et al.*, Nature Comm. **4**, 1527 (2013).
[26] A. I. Kuznetsov *et al.*, Science **354**, aag2472 (2016).
[27] P. Woźniak, P. Banzer, *et al.*, Laser Phot. & Rev. **9**, 231 (2015).
[28] T. Das, P. P. Iyer, R. A. DeCrescent, and J. A. Schuller, Phys. Rev. B **92**, 241110(R) (2015).
[29] Z. Xi, L. Wei, *et al.*, Optics Lett. **41**, 33 (2016).
[30] L. Wei, N. Bhattacharya, and H. P. Urbach, Optics Lett. **42**, 1776 (2017).
[31] W. Liu and Y. S. Kivshar, Optics Expr. **26**, 13085 (2018).
[32] M. F. Picardi, A. V. Zayats, and F. J. Rodríguez-Fortuño, Phys. Rev. Lett. **120**, 117402 (2018).
[33] K. Y. Bliokh, D. Smirnova, and F. Nori, Science **348**, 1448 (2015).
[34] L. Wei *et al.*, Optics Lett. **43**, 3393 (2018).
[35] J. Xiang *et al.*, Laser Phot. & Rev. **12**, 1800032 (2018).
[36] M. Nieto-Vesperinas and J. J. Saenz, Optics Lett. **35**, 4078 (2010).
[37] K. Y. Bliokh *et al.*, Nature Comm. **5**, 3300 (2014).
[38] D. Li, L. Shao, *et al.*, Science **349**, 6251 (2015).
[39] M. Nieto-Vesperinas *et al.*, Optics Expr. **18**, 11428 (2010).
[40] J. M. Geffrin *et al.*, Nature Comm. **3**, 1171 (2012).
[41] C. F. Bohren and D. R. Huffman, Absorption and Scattering of Light by Small Particles, Wiley-VCH (1998).
[42] M. F. Picardi, A. Manjavacas, A. V. Zayats, and F. J. Rodríguez-Fortuño, Phys. Rev. B **95**, 245416 (2017).